Cell Reports, Volume *33*

Supplemental Information

4EHP and GIGYF1/2 Mediate Translation-Coupled Messenger RNA Decay

Ramona Weber, Min-Yi Chung, Csilla Keskeny, Ulrike Zinnall, Markus Landthaler, Eugene Valkov, Elisa Izaurralde, and Cátia Igreja

Weber *et al.* Figure S1

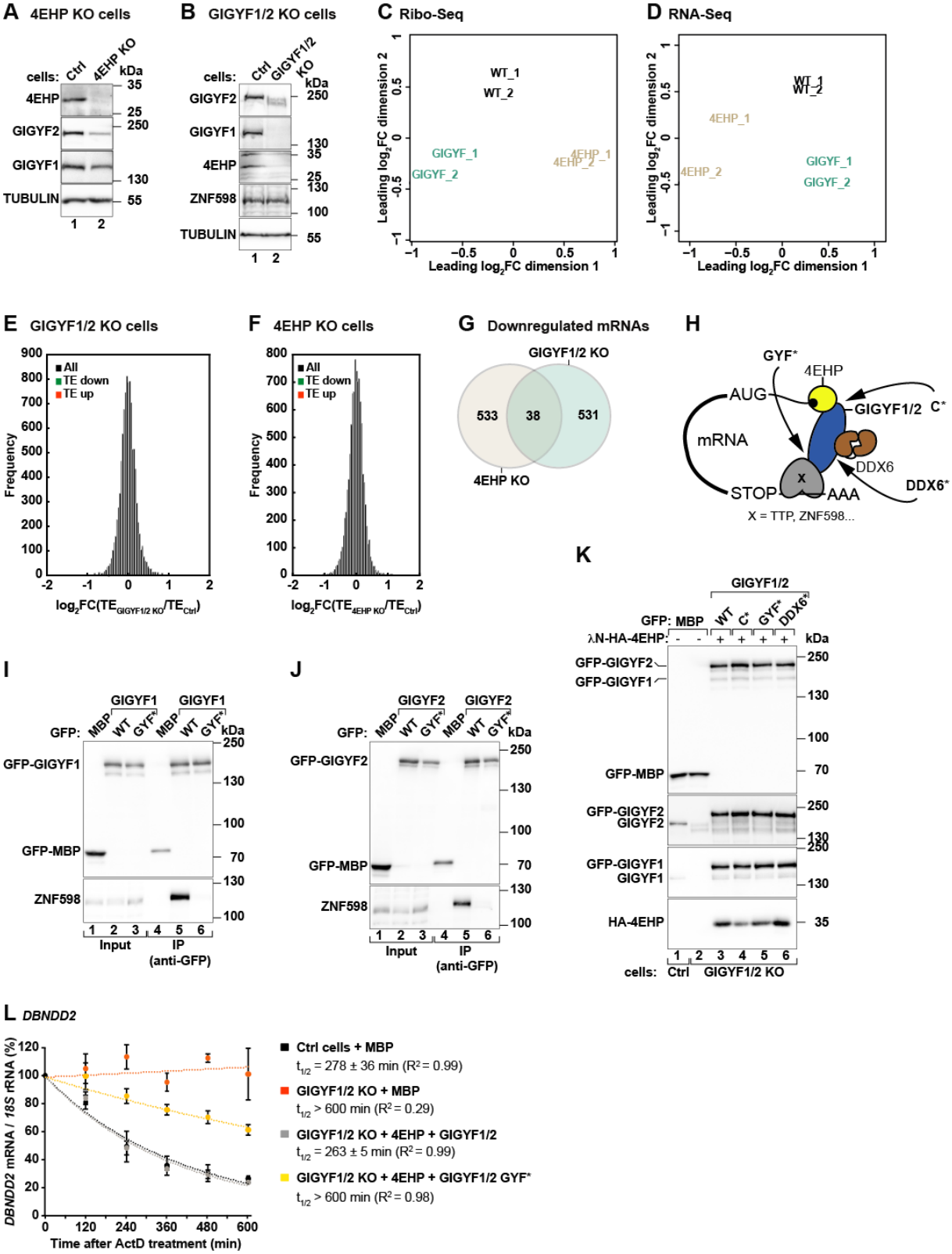

Figure S1, related to Figures 1 and 3. Characterization of 4EHP-null (KO) and GIGYF1/2-null cells

(A, B) Western blots demonstrating loss of endogenous 4EHP in 4EHP KO cells (A) and endogenous GIGYF1 and GIGYF2 in GIGYF1/2 KO cells (B). GIGYF1 and GIGYF2 expression is reduced in 4EHP KO cells and

4EHP is weakly expressed in GIGYF1/2 KO cells. TUBULIN served as loading control. Note that the TUBULIN antibody recognizes an epitope common among the α-tubulin subunits of which TUBA4A and TUBA1A are genes with increased mRNA abundance in 4EHP-null cells.

(C, D) Multidimensional scaling (MDS) analysis for the Ribo-Seq replicate libraries (C) and the RNA-Seq replicate libraries (D) from HEK293T WT, GIGYF1/2-null and 4EHP-null cells.

(E, F) Histograms of the number of transcripts (frequency) relative to the $\log_2$FC of translational efficiency (TE) in GIGYF1/2 null (E) and 4EHP null cells (F). Significantly upregulated (FDR<0.005 and $\log_2$FC>0) transcripts are depicted in orange, significantly downregulated (FDR<0.005 and $\log_2$FC<0) transcripts are shown in green. There were only few genes with changes in TE (Table S1).

(G) Venn diagram of the genes with decreased mRNA abundance (downregulated genes) in GIGYF1/2 null and 4EHP null cells identifies a non-significant overlap of 38 transcripts.

(H) Schematic representation of the effector complex involved in GIGYF1/2-mediated mRNA decay. GIGYF1/2 canonical (C*) mutant is unable to interact with 4EHP; GIGYF1/2 DDX6* protein does not associate with the RNA helicase DDX6; the GIGYF1/2 GYF* mutant cannot interact with PPGΦ-rich proteins. TTP: tristetraprolin; X: RNA-binding protein.

(I, J) The interaction of GIGYF1 (I) and GIGYF2 (J) WT or GYF domain mutant (GYF*) with ZNF598 was analyzed in co-immunoprecipitation assays using anti-GFP antibodies. GFP-MBP served as a negative control. The input (0.8% for the GFP proteins and 0.3% for ZNF598) and immunoprecipitated fractions (12% for the GFP proteins and 24% for ZNF598) were analyzed by western blotting with anti-GFP and anti-ZNF598 antibodies.

(K) Immunoblot showing the expression of the proteins used in the experiment depicted in Figures 3A, B. Blots were probed with antibodies recognizing GFP, GIGYF1, GIGYF2 or HA. Inputs and immunoprecipitates were 2% and 2.7%, respectively.

(L) Ctrl and GIGYF1/2 KO cells were transfected with plasmids expressing λN-HA or λN-HA-4EHP, GFP-MBP, and GFP-GIGYF1/2 (WT or GYF*). Two days post transfection, cells were treated with ActD and harvested at the indicated time points. *DBNDD2* mRNA levels were quantified by qRT-PCR and normalized to those of *18S* rRNA. Circles represent the mean value; error bars represent SD (n=3). The decay curves were fitted to an exponential decay with a single component (dotted lines). R^2 values are indicated for each curve.

Weber *et al.* Figure S2

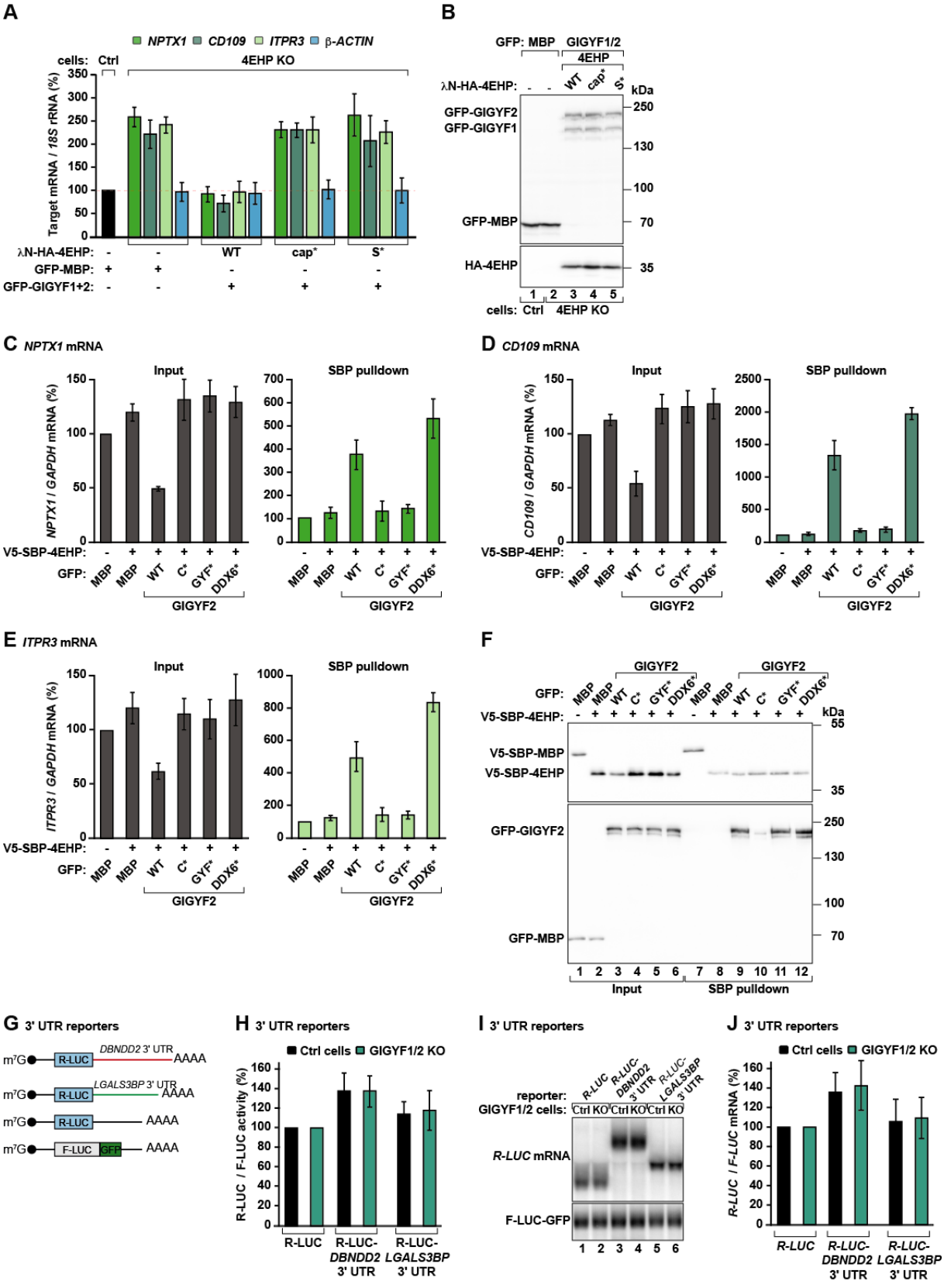

Figure S2, related to Figure 3. Binding of 4EHP to the cap and to GIGYF1/2 is crucial for mRNA decay.

(A) Control and 4EHP null cells were transfected with plasmids expressing λN-HA alone, wild type (WT) or the indicated λN-HA-4EHP mutants (cap-binding mutant: cap*, GIGYF1/2 specific-binding mutant: S*), GFP-

MBP or GFP-GIGYF1 and GFP-GIGYF2. *NPTX1*, *CD109*, *ITPR3* and *β-ACTIN* mRNA levels were determined by qRT-PCR and normalized to that of *18S* rRNA in the presence of the different 4EHP proteins. Bars represent the mean values and error bars denote the SD of three independent experiments.

(B) Western blot showing the expression levels of the proteins used in the experiments shown in (A). Blots were probed with anti-GFP and anti-HA antibodies.

(C-F) HEK293T cells were transfected with plasmids expressing V5-SBP-MBP or V5-SBP-4EHP, GFP-MBP or GFP-GIGYF2 (WT or mutants). Streptavidin binding protein-based pulldowns were performed two days post transfection and protein and RNA samples were collected for each experimental condition. *NPTX1*, *CD109* and *ITPR3* mRNA levels in input (0.8%) and IP samples (12%) were quantified by qRT-PCR, normalized over *GAPDH* and set to 100% in the presence of V5-SBP-MBP. Bars represent the mean value; error bars represent standard deviations from three independent experiments. (F) Western blot showing the expression of the proteins in the inputs (1% for the V5-SBP-tagged proteins and 0.5% for GFP-tagged proteins) and bound fractions (0.9% for the V5-SBP-tagged proteins and 2.7% for GFP-tagged proteins) from the experiments described in C-E.

(G) Schematic representation of the *DBNDD2* and *LGALS3BP* 3′ UTR reporters. *Renilla* luciferase (R-LUC); firefly luciferase (F-LUC); green fluorescent protein (GFP).

(H-J) Ctrl and GIGYF1/2 KO cells were transfected with the R-LUC-*DBNDD2*-3′ UTR, the R-LUC-*LGALS3BP*-3′ UTR or the R-LUC reporters and the transfection control F-LUC-GFP. (H) R-LUC activity was normalized to that of F-LUC-GFP and set to 100% for R-LUC in each cell line. (I) mRNA levels were determined by northern blotting. (J) *R-LUC*, *R-LUC-DBNDD2*-3′ UTR and *R-LUC-LGALS3BP*-3′ UTR band intensities were normalized to the intensity of *F-LUC-GFP* mRNA band and set to 100% for the R-LUC reporter in each cell line.

Weber *et al.* Figure S3

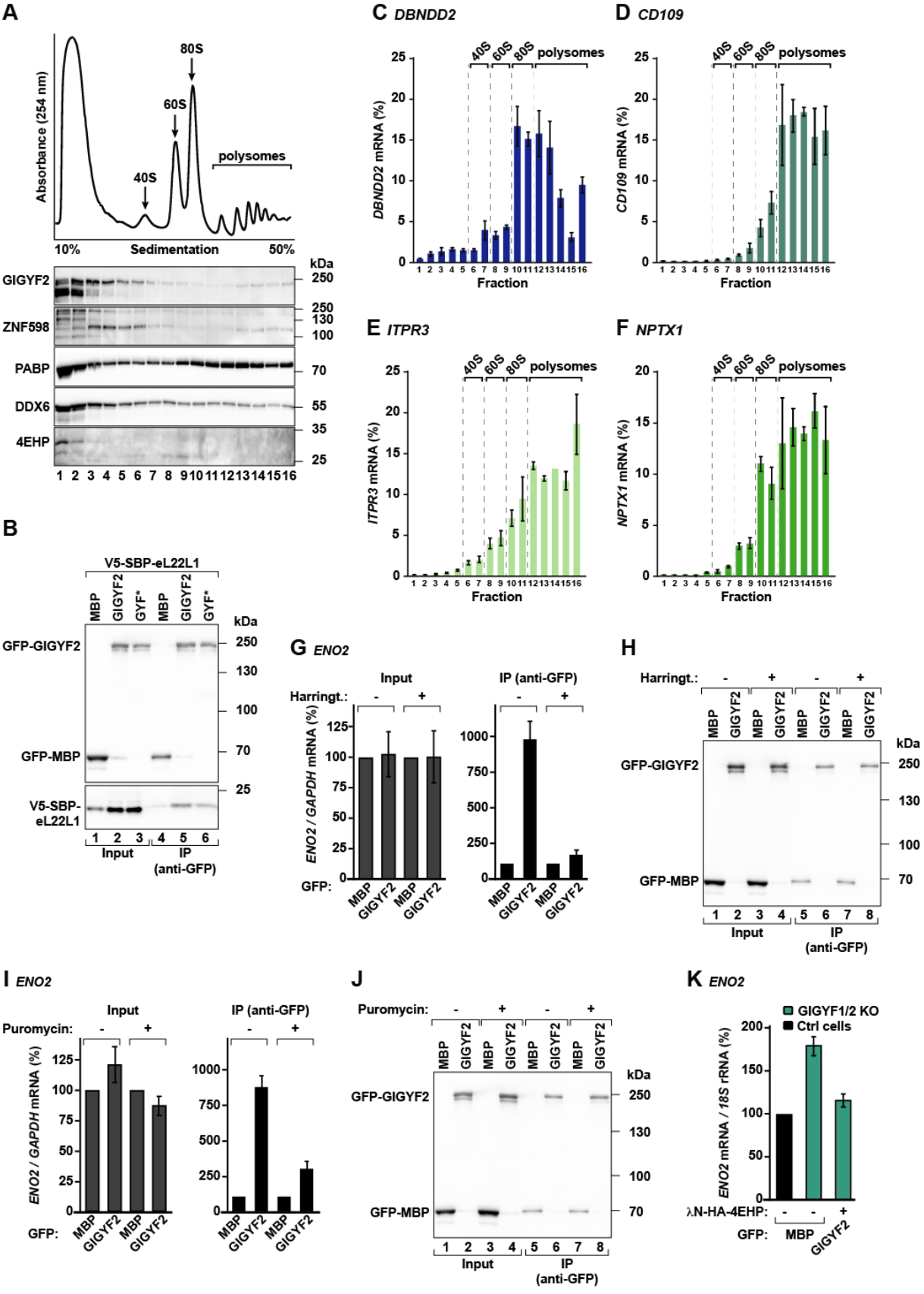

Figure S3, related to Figure 4. GIGYF1/2 promote decay of actively translating mRNAs

(A) UV absorbance profile at 254 nm of HEK293T cell extracts after polysome sedimentation in a sucrose gradient. 40S and 60S subunits, 80S monosomes, and polysome peaks are indicated. The distribution of GIGYF2, ZNF598, PABP, DDX6 and 4EHP across the gradient was analyzed by western blotting and is depicted below the profile.

(B) Immunoblot showing the interaction of GFP-GIGYF2 with V5-SBP-eL22L1 ribosomal protein. Proteins were immunoprecipitated using anti-GFP antibodies. GFP-MBP served as a negative control. The input (0.8% for the GFP proteins and 0.1% for V5-SBP-eL22L1) and immunoprecipitated fractions (12% for the GFP proteins and 24% for V5-SBP-eL22L1) were analyzed by western blotting with anti-GFP and anti-V5 antibodies.

(C-F) Abundance profiles for *DBNDD2*, *CD109*, *ITPR3* and *NPTX1* along the density gradient. mRNA levels were determined by qRT-PCR in samples prepared from total RNA extracted from each sucrose fraction. Bars represent the mean value; error bars denote the standard deviations from three independent experiments.

(G-J) HEK293T transfected with GFP-MBP or GFP-GIGYF2 were incubated with DMSO and the translational inhibitors harringtonine (G, H) or puromycin (I, J). After cell lysis, proteins were immunoprecipitated using anti-GFP antibodies. Protein and RNA samples were obtained for each experimental condition. Input (2%) and immunoprecipitated fractions (2.7%) were analyzed by western blotting. RNA samples were reversed transcribed and *ENO2* expression levels in input (0.8%) and IP samples (12%) were quantified by qRT-PCR, normalized to *GAPDH* and set to 100% in the presence of GFP-MBP. Bars represent the mean value and error bars the standard deviations from three independent experiments.

(K) Control and GIGYF1/2-null cells were transfected with plasmids expressing GFP-MBP or GFP-GIGYF2 and λN-HA-4EHP. RNA samples were collected and *ENO2* mRNA levels were quantified by qRT-PCR. mRNA levels were normalized to that of *18S* rRNA and set to 100% in Ctrl cells.

Weber *et al.* Figure S4

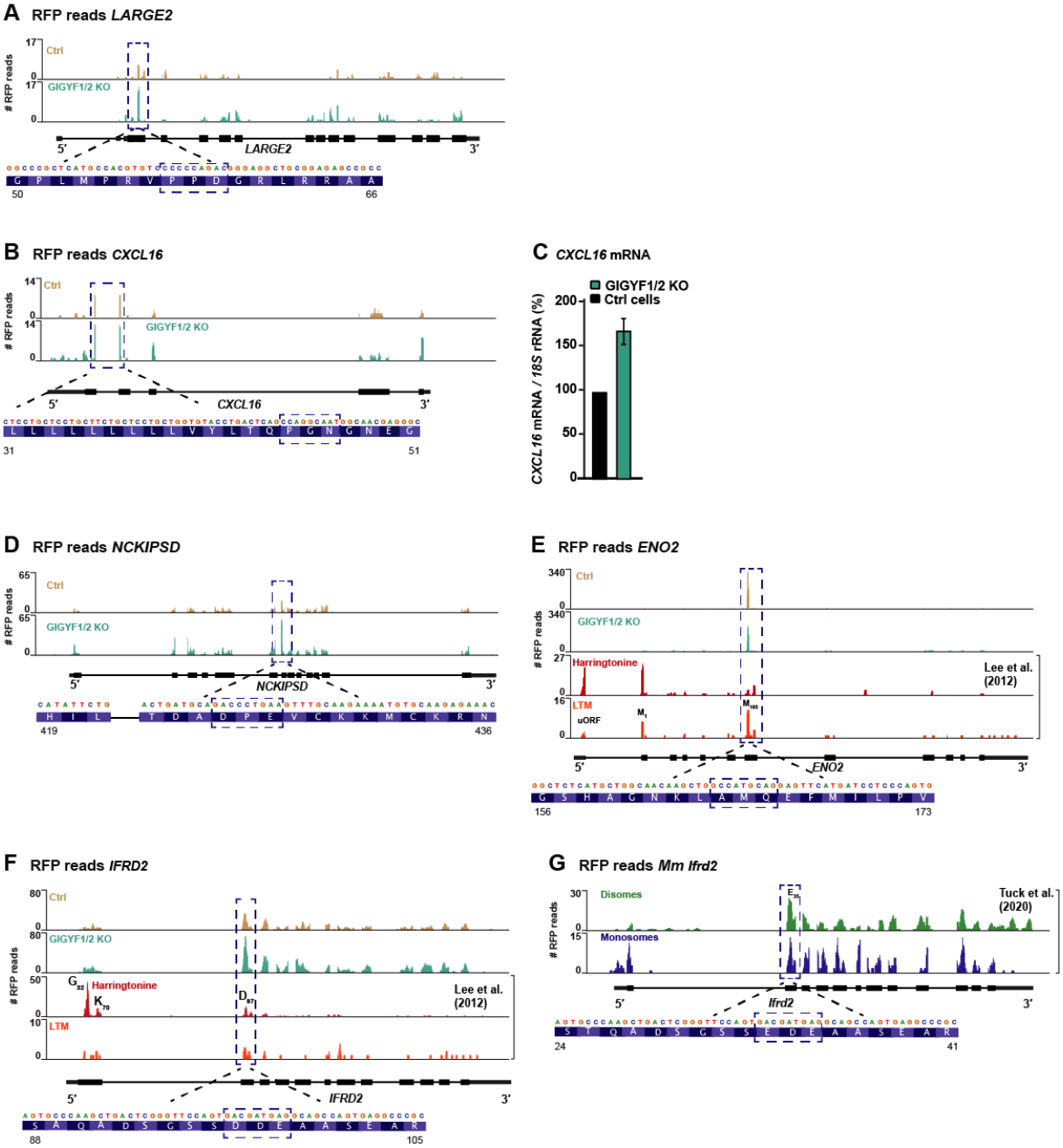

Figure S4, related to Figure 5. Ribosome density profiles in GIGYF1/2–4EHP target mRNAs reveal translational pausing

(A, B) Ribosome density profiles on *LARGE2* and *CXCL16*. The dashed blue box indicates the ribosome pause site. The nucleotide, peptide sequence at the pause site and residue numbering are depicted below the profiles.

(C) *CXCL16* mRNA steady state levels were quantified by qRT-PCR in control (Ctrl) and GIGYF1/2 null (KO) cells. mRNA levels were normalized to that of *18S* rRNA and set to 100% in Ctrl cells.

(D, E) Distribution of RFPs across the CDS of *NCKIPSD* and *ENO2* in Ctrl and GIGYF1/2 KO cells. Translational stalls with increased RFPs are highlighted with a dashed blue box. For *ENO2*, RFP distribution in

cells treated with the translational inhibitors harringtonine and lactimidomycin (LTM) obtained by Lee and co-workers (Lee et al., 2012) are also shown. Transcript organization, nucleotide and peptide sequence at the pause site, and residue numbering are depicted below the profiles. Upstream open reading frame (uORF), Met_1 (M_1), Met_{165} (M_{165}).

(F) RFPs distribution along the CDS of *IFRD2* in Ctrl, GIGYF1/2 KO, harringtonine- and LTM-treated cells (Lee et al., 2012). In cells treated with harringtonine, RFPs are observed at different positions of *IFRD2*; one of these corresponds to the paused ribosome at the DDE motif observed in this study. Transcript organization, nucleotide and peptide sequence at the pause site, and residue numbering are depicted below the profiles. Gly_{32} (G_{32}), Lys_{70} (K_{70}), Asp_{97} (D_{97}).

(G) Monosome and disome footprint distribution in *Mus musculus* (*Mm*) *Ifrd2*, as determined by Tuck and co-workers (Tuck et al., 2020). Of note is the occurrence of disomes at an equivalent position of the pause peptide observed in the human orthologue transcript. Transcript organization, nucleotide and peptide sequence at the pause site, and residue numbering are depicted below the profiles. Glu_{35} (E_{35}).

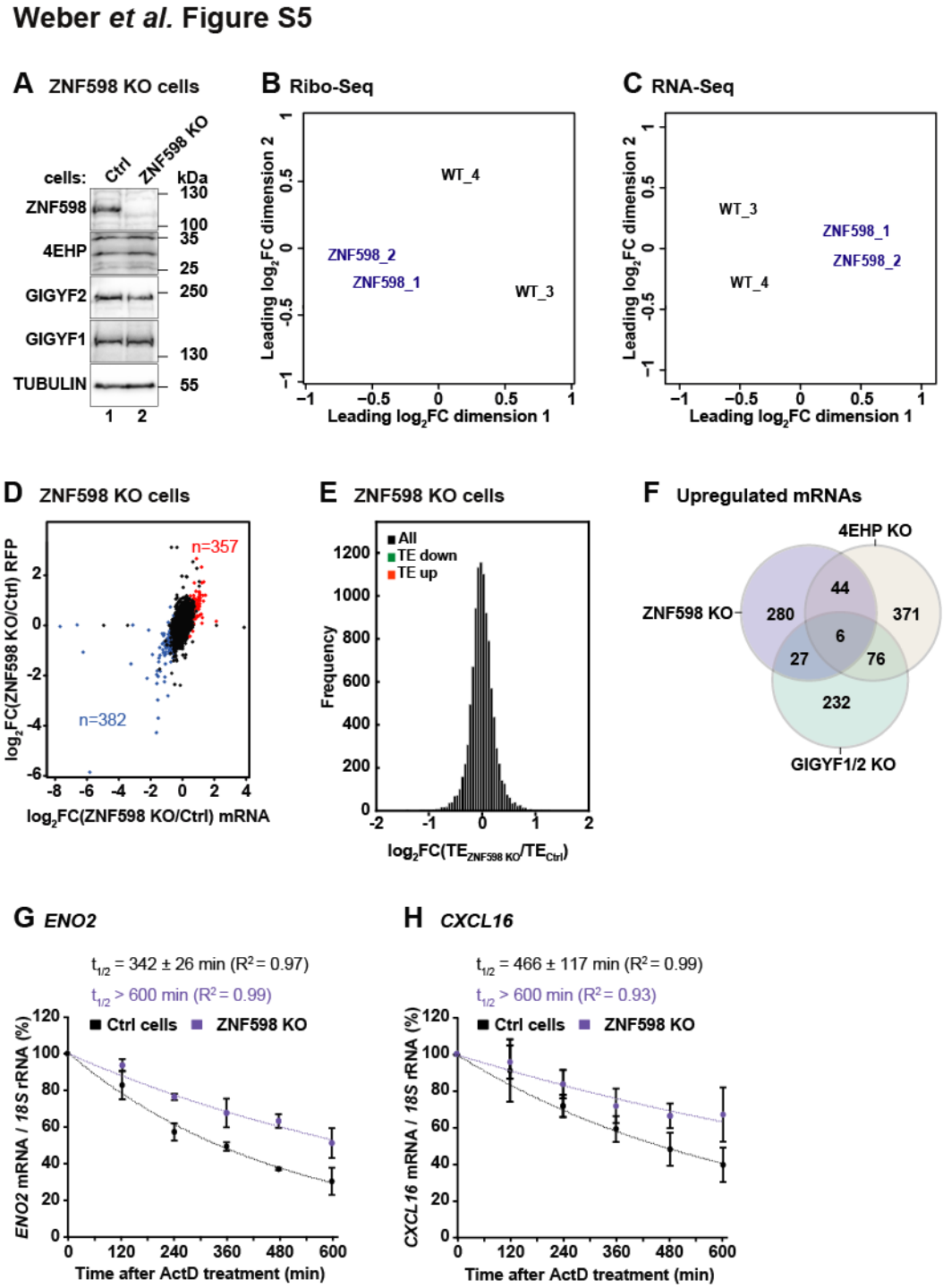

Figure S5, related to Figure 1. The ubiquitin ligase ZNF598 is only required for co-translational decay of a fraction of GIGYF1/2 targets

(A) Immunoblot showing the lack of ZNF598 expression in the null cells. 4EHP and GIGYF1/2 expression does not vary in ZNF598 null cells. TUBULIN was used as a loading control.

(B, C) Multidimensional scaling (MDS) analysis for the Ribo-Seq replicate libraries (B) and the RNA-Seq replicate libraries (C) from HEK293T WT and ZNF598 null cells.

(D) Genome-wide assessment of changes in RFPs and mRNA abundance in ZNF598 KO cells, depicted on a $\log_2$ scale. Each dot represents an individual gene (n_{total}=10453) with FPKM>2. In ZNF598 KO cells, 357 genes were significantly upregulated (FDR<0.005 and $\log_2$FC>0; red), whereas 382 genes were significantly downregulated (FDR<0.005 and $\log_2$FC<0; blue).

(E) Histogram showing the number of transcripts (frequency) in ZNF598 null cells with changes in TE ($\log_2$FC) relative to Ctrl cells. Transcripts with increased TE (n=5) in the absence of ZNF598 are shown in orange (FDR<0.005 and $\log_2$FC>0), whereas less translated transcripts (n=2) are depicted in green (FDR<0.005 and $\log_2$FC<0). See also Table S1.

(F) Venn diagram of the genes with increased mRNA abundance (upregulated genes) in ZNF598 null, GIGYF1/2 null and 4EHP null cells.

(G, H) Ctrl and ZNF598 KO HEK293T cells were treated with Actinomycin D (ActD) and harvested at the indicated time points. *ENO2* and *CXCL16* transcript levels were assessed by qRT-PCR and normalized to that of *18S* rRNA. The normalized value at time zero (before ActD addition) was defined as 100%. Results were plotted as a function of time post ActD addition. Circles represent the mean value; error bars represent the SD from three independent experiments. The decay curves were fitted to an exponential decay with a single component (dotted lines). R^2 values are indicated for each curve. The half-life of each mRNA in Ctrl (black) and null (purple) cells is represented as the mean +/- SD.

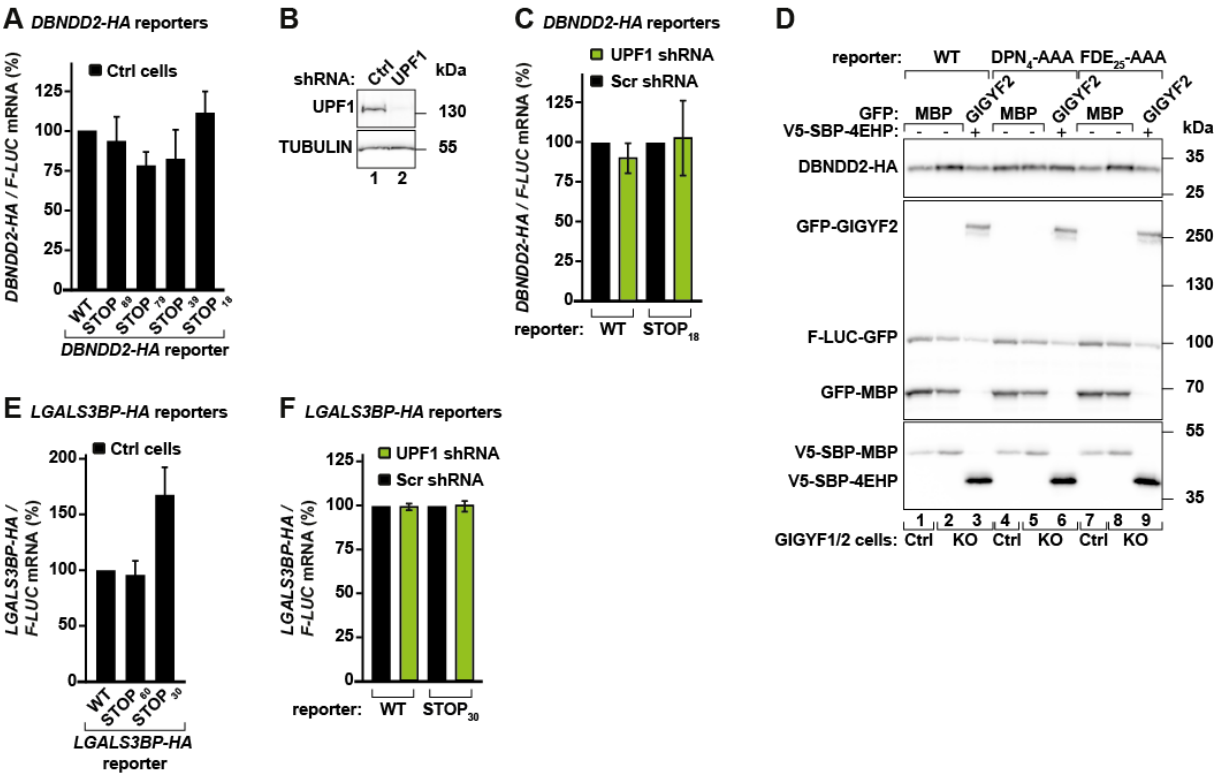

Figure S6, related to Figure 5. Wild type and mutant target-based CDS reporters

(A) Comparison of *DBNDD2-HA* (WT or $STOP_x$) reporter levels in HEK293T cells, as assessed by northern blotting (see Figure 5C). mRNA levels were normalized to *F-LUC-GFP* and set to 100% for the WT reporter. Bars represent the mean values and error bars denote the SD of three independent experiments.

(B) Western blot showing shRNA-mediated depletion of UPF1 in HEK293T cells. TUBULIN served as a loading control.

(C) HEK293T cells were treated with scramble (Scr) or shRNA targeting *UPF1* mRNA and transfected with *DBNDD2-HA* (WT or $STOP_{18}$) and *F-LUC-GFP*. The graph shows *DBNDD2-HA* mRNA abundance in control (Scr) and UPF1 KD cells. mRNA levels were determined by qRT-PCR, normalized to that of *F-LUC-GFP* and set to 100% in Scr-treated cells.

(D) Ctrl and GIGYF1/2-null cells were transfected with WT or mutant *DBNDD2-HA* plasmids. Protein samples were analyzed by western blotting using anti-V5, anti-HA and anti-GFP antibodies.

(E) Quantification of *LGALS3BP-HA* (WT or $STOP_x$) mRNA levels in HEK293T cells. RNA samples were analyzed by RT-qPCR (see Figure 6C). mRNA levels were normalized to *F-LUC-GFP* and set to 100% for the WT reporter. Bars represent the mean values and error bars denote the SD of three independent experiments.

(F) HEK2933T cells treated with Scr or UPF1 shRNAs were transfected with *LGALS3BP-HA* (WT or $STOP_{30}$) and *F-LUC-GFP*. *LGALS3BP-HA* mRNA levels were determined by RT-qPCR, normalized to that of *F-LUC-GFP* and set to 100% in Scr-treated cells.

Weber *et al.* Figure S7

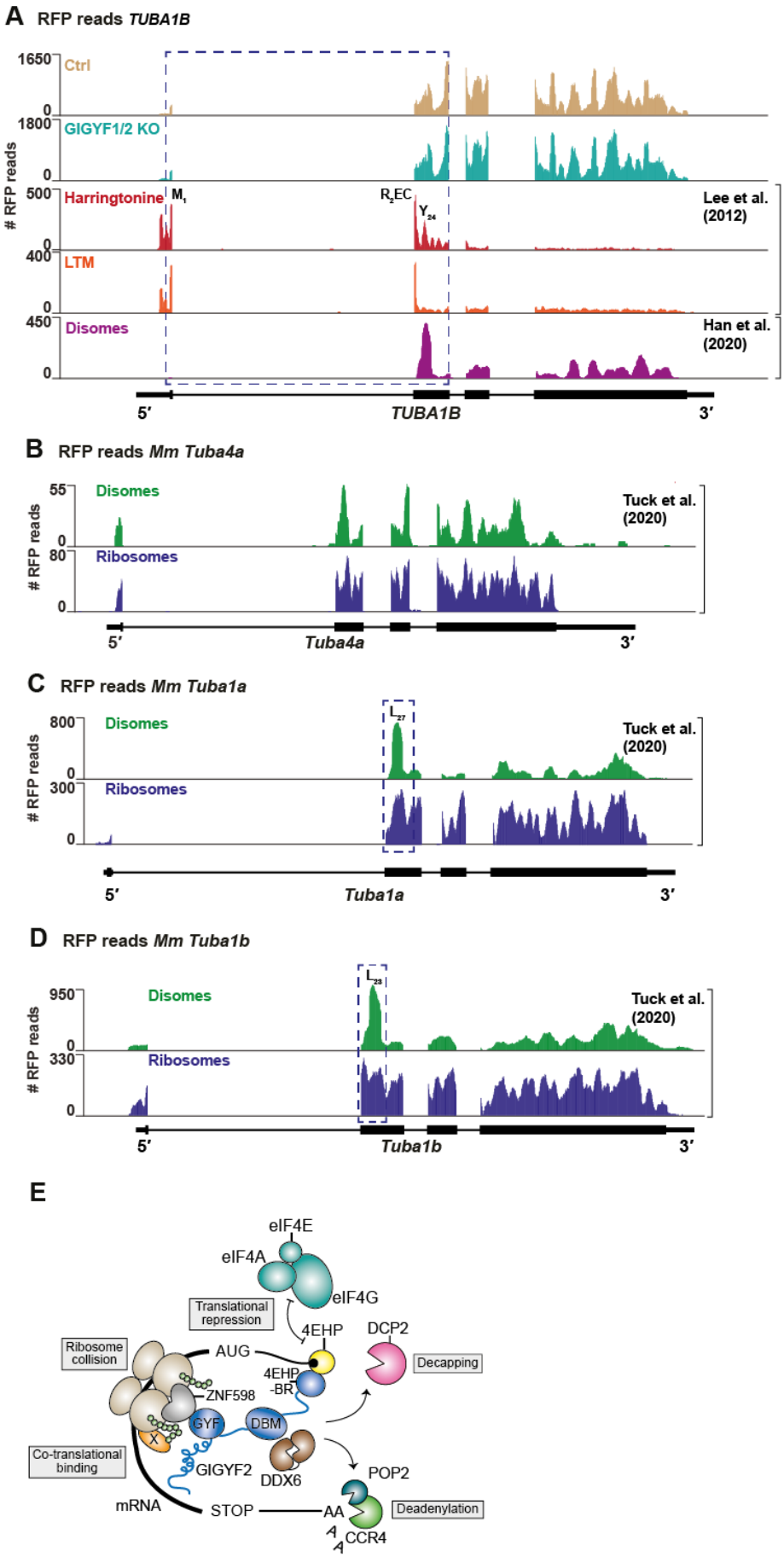

Figure S7, Related to Figure 7. Monosome and disome density profiles in *TUBULIN* mRNAs reveal translational pausing

(A) RFP of *TUBA1B* in Ctrl, GIGYF1/2 KO, and cells treated with harringtonine or lactimidomycin (LTM) as determined by Lee and co-workers (Lee et al., 2012). Harringtonine footprints identify the initiating ribosome at the translation start site (M_1) and paused elongating ribosomes (dashed blue square). The profile also shows the distribution of disome footprints along the CDS in HEK293 cells as obtained by Han and co-workers (Han et al., 2020). Met_1 (M_1); Arg_2 (R_2), Glu (E), Cys (C), Tyr_{24} (Y_{24}). Transcript UTRs, intron and exons are depicted below the profiles.

(B-D) Monosome and disome density profiles of *Mm Tuba1a*, *Tuba4a* and *Tuba1b* transcripts based on the data previously obtained by Tuck and co-workers in mouse embryonic stem cells (Tuck et al., 2020). The dashed blue box indicates the occurrence of ribosome collision (disomes) in the first 20-30 codons of tubulins. Transcript UTRs, intron and exons are depicted below the profiles.

(E) Recruitment of 4EHP-GIGYF1/2 complexes to transcripts with perturbed elongation induces translation repression, mRNA deadenylation and decapping. 4EHP, in yellow, competes with eIF4F (eIF4E+eIF4G+eIF4A) for cap-binding, blocking translation and promoting decapping. Binding of 4EHP to the mRNA depends on GIGYF1/2 proteins (in blue), the scaffolds of the repressor complexes. mRNA selection involves the recognition of paused ribosomes by factors such as the E3 ubiquitin ligase ZNF598 (in grey), which binds to the GYF domain of GIGYF1/2. In addition, target selection can be favored by co-translational binding of components of the surveillance machinery (X) to the nascent peptide chain. Recognition of the nascent chain by specific factors (X), or the synthesis of the nascent peptide itself, might then interfere with ribosome activity, causing ribosome pausing and collisions. Detection of such events coupled to the recruitment of 4EHP and GIGYF1/2, exposes the translating mRNA to degradation. GIGYF1/2 also recruit the RNA helicase DDX6 which is required for target repression and decay. Altogether, GIGYF1/2 initiate a series of events that irrevocably prevent the translation of mRNAs with impaired elongation. DCP2: decapping enzyme 2; POP2 and CCR4: deadenylases; 4EHP-BR: 4EHP-binding region; DBM: DDX6-binding motif.

Table S6. Genes commonly upregulated in ZNF98 null, GIGYF1/2 null and 4EHP null HEK293T cells. Related to Figure 1.

ZNF598 null and GIGYF1/2 null cells	ZNF598 null and 4EHP null cells
Gene name	**Gene name**
ABCA3	AACS
AIFM2	ALG1L
AMIGO1	APOBEC3B
APOL2	APOE
BASP1	ARHGEF2
BEX5	ARHGEF6
CCDC88C	ARMCX5-GPRASP2
CHRDL1	ATF3
COL1A1	CLU
CXCL16	CSTF2T
CYP2J2	CXCL16
EHD2	CYR61
ENO2	DDR2
HLA-DPA1	DIAPH3
IFI6	DNMT1
IFIH1	EEF1A2
IFIT5	EIF2AK2
IFITM1	EMP3
KIF1A	ENO2
KRT18	FLNA
MGST1	FLNC
MLLT11	GPRASP2
NDRG1	HLA-DPA1
NELL2	IFITM2
NQO1	JUN
PLEKHG4	KHK
PSMB9	KIF1A
RHOB	KLF10
TCEAL3	LPIN1
TP53I3	MAP1B
TRIB1	MED12
TRIM47	MRC2
UBE2L6	MSH2
	OPTN
	PDE7A
	PDP1
	PLEKHA2
	PLEKHG4
	PLEKHH3
	PTRF
	RAB3GAP2
	RAB6B
	RNF213
	SLAIN1
	TBC1D32
	TCEAL3
	TNFRSF12A
	TRIM25
	TTLL7
	TUBB4A

Table S7. primers used in this study. Related to STAR Methods.

		sequence (5' to 3')
qPCR		
DBNDD2	fwd	CCAGCAGCTCCGCCTTC
	rev	GTTGTCCACCCCAGACGAC
CD109	fwd	GGTTGAGGAGCATACTGAAAAT
	rev	TGGCAGTCTAATGCTCACACCC
NPTX1	fwd	TCTGCAGGGATCTTCTCCGTTT
	rev	TCCCAGCTGTGGGAATCCTTTA
ITPR3	fwd	CTGCTGCATTTGTGGACACCTG
	rev	CACTACGCAGGTCAGCGAAGGT
ENO2	fwd	ATGTGTCACTTGTGCTTTGCTC
	rev	ACCCCAGTCATCTTGGGATCTA
CXCL16	fwd	CTCCAGATCTGCCGGTTCATTA
	rev	ATCACCCAGTGTGAAAAGCAGA
TUBA4A	fwd	TGAAACTGGTGCTGGAAAACAC
	rev	CTCCATCAGGAGTGAGGTGAAG
TUBB4A	fwd	CTCGAGGCTTCTGACCTTTGAT
	rev	TTAAAGGTGCGGTTTCCAGAGT
TUBA1A	fwd	CCACAGTCATTGATGAAGTTCG
	rev	GCTGTGGAAAACCAAGAAGC
TUBA1B	fwd	AATTCGCAAGCTGGCTGA
	rev	CGACAGATGTCATAGATGGCC
TUBB	fwd	GAAGCCACAGGTGGCAAATA
	rev	CGTACCACATCCAGGACAGA
GAPDH	fwd	CTCTGCTCCTCCTGTTCGACAG
	rev	TTCCCGTTCTCAGCCTTGACGG
β-ACTIN	fwd	GCAGGAGTATGACGAGTCCGGC
	rev	GTAACAACGCATCTCATATTTG
18S rRNA	fwd	CAGCCACCCGAGATTGAGCA
	rev	TAGTAGCGACGGGCGGTGTG
LGALS3BP-HA	fwd	CTGGGCCTCACCAAGTCTGGCG
	rev	AGCGTAATCTGGAACATCGTAT
DBNDD2-HA	fwd	CCAGCAGCTCCGCCTTC
	rev	AGCGTAATCTGGAACATCGTAT
sgRNA		
sg4EHP-a	TATAGCCACATGGTACGTCC	
sg4EHP-b	TGTTTTCTTCATTCTGATCA	
sgZNF598	CTACTGCGCCGTGTGCCGCG (Garzia et al., 2017)	
sgZNF598	GAAAGGTGTACGCATTGTAC (Garzia et al., 2017)	
shRNA		
Scramble	ATTCTCCGAACGTGTCACG (Jonas et al., 2013)	
UPF1-I	GAGAATCGCCTACTTCACT (Paillusson et al., 2005)	
UPF1-II	GATGCAGTTCCGCTCCATT (Paillusson et al., 2005)	
Ribosome profiling		

30 nt RNA marker	AUGUACACGGAGUCGAGCUCAACCCGCAAC-P
27 nt RNA marker	AUGUACACGGAGUCGAGCUCAACCCGC-P
3' adapter	rApp/NNNNT GGA ATT CTC GGG TGC CAA GG/3InvdT/
5' adapter (RNA)	GUUCAGAGUUCUACAGUCCGACGAUCNNNN
Reverse transcription primer	GCCTTGGCACCCGAGAATTCCA
Forward primer	AATGATACGGCGACCACCGAGATCTACACGTTCAGAGTT CTACAGTCCGA
Barcoded reverse primer	CAAGCAGAAGACGGCATACGAGATNNNNNNGTGACTGG AGTTCCTTGGCACCCGAGAATTCCA